



ORIGINAL RESEARCH



High expression of PD-1 and PD-L1 in ocular adnexal sebaceous carcinoma

Thomas J. Kandl^{#a}, Oded Sagiv ^{#a}, Jonathan L. Curry^{b,c}, Jing Ning^d, Junsheng Ma^d, Courtney W. Hudgens ^e, John Van Arnam^b, Jennifer A. Wargo^f, Bitá Esmali^{a*}, and Michael T. Tetzlaff^{b,e*}

^aOrbital Oncology and Ophthalmic Plastic Surgery, Department of Plastic Surgery, The University of Texas MD Anderson Cancer Center, Houston, Texas, USA; ^bDepartment of Pathology, Section of Dermatopathology, The University of Texas MD Anderson Cancer Center, Houston, Texas, USA; ^cDepartment of Dermatology, The University of Texas MD Anderson Cancer Center, Houston, Texas, USA; ^dDepartment of Biostatistics, The University of Texas MD Anderson Cancer Center, Houston, Texas, USA; ^eDepartment of Translational and Molecular Pathology, The University of Texas MD Anderson Cancer Center, Houston, Texas, USA; ^fDepartment of Surgical Oncology, The University of Texas MD Anderson Cancer Center, Houston, Texas, USA

ABSTRACT

Ocular adnexal sebaceous carcinoma (OASC) is an aggressive malignancy that frequently recurs locally and metastasizes. Surgical extirpation may produce significant aesthetic morbidity, and effective systemic therapies for locally advanced or metastatic disease are largely ineffective. Immune checkpoint inhibitors have shown efficacy in the management of several solid tumors where tumor cell PD-L1 expression correlates with improved response. To determine whether OASC might be amenable to immune checkpoint blockade, we performed comprehensive immune profiling for CD3, CD8, PD-1, FOXP3, and PD-L1 in 24 patients with primary OASC. The composition, distribution and density of the tumor associated immune infiltrate were quantified by automated image analysis and correlated with measures of clinical outcome. Tumor cells in 12 OASCs (50%) expressed PD-L1. Higher densities of CD3+ ($p = 0.01$), CD8+ ($p = 0.006$), and PD-1+ ($p = 0.024$) tumor-associated T cells were associated with higher T category ($\geq T3a$ per the 7th edition of the American Joint Committee on Cancer staging manual). Higher tumor cell expression of PD-L1 correlated with higher density of PD-1+ tumor-associated T cells ($p = 0.021$). Since a CD3+ CD8+ PD-1 + T-cell infiltrate represents a “suppressed T-cell phenotype” apparently permissive toward OASC progression, our findings provide a mechanistic rationale for the effective application of immune checkpoint blockade in OASC to abrogate PD-1/PD-L1 interaction and effectively unleash the immune infiltrate to treat higher-stage tumors.

ARTICLE HISTORY

Received 11 April 2018
Revised 5 May 2018
Accepted 7 May 2018

KEYWORDS



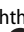

Sebaceous; carcinoma; ocular; PD-L1; PD-1; biomarkers; immunosurveillance; inflammation and cancer

Introduction

Ocular adnexal sebaceous carcinoma (OASC) is an aggressive malignant neoplasm originating from the sebaceous glands in the periocular region.^{1,2} OASC represents the second most common eyelid malignancy in the United States, accounts for 5% of all eyelid malignancies.^{3,4} Sebaceous carcinoma is most frequently seen in the periocular region, with the eyelid and conjunctiva being the most common sites.⁵⁻⁷ Many features contribute to the aggressive clinical course of OASC. First, OASC clinically mimics more common inflammatory eyelid conditions, such as blepharconjunctivitis and chalazion; thus, definitive diagnosis is delayed in up to 50% of patients.^{1,8,9} Furthermore, OASC exhibits discontinuous intraepithelial extension together with a locally infiltrative growth pattern, and in 13% to 23% of patients, orbital exenteration is required to achieve local control, resulting in significant functional and aesthetic morbidity.⁸⁻¹¹ One of the largest studies of OASC to date showed that at diagnosis, 18% of patients had regional nodal metastasis and 8% had distant metastasis.¹² Systemic

therapies for regional or distant metastases, however, remain largely ineffective, and 6% to 22% of patients with OASC die of the disease.^{8,10,12} Together, these observations underscore an ongoing critical need to identify novel efficacious therapies to achieve better control of both local and metastatic disease.

An emerging approach in cancer therapy is to exploit the programmed death protein-1 (PD-1)/programmed death ligand-1 (PD-L1) immune checkpoint blockade pathway to activate the immune system to destroy tumor cells. PD-L1 is endogenously expressed by immune cells and stromal cells. PD-1, the primary ligand of PD-L1, is expressed by T cells. Engagement of PD-1 with PD-L1 elicits inhibitory signals delivered to T cells, culminating in a dampened immune response. This pathway serves to avert excessive immune stimulation and subsequent collateral tissue injury.^{13,14} Some tumor types co-opt PD-L1 expression and therefore exploit endogenous immune checkpoint pathways to evade eradication by the immune system. Immune checkpoint inhibitors (anti-PD-1 and anti-PD-L1 antibodies) abrogate the PD-1/PD-L1 interaction to promote prolonged activation of the

CONTACT Bitá Esmali  besmaeli@mdanderson.org  Orbital Oncology and Ophthalmic Plastic Surgery, Department of Plastic Surgery, Unit 1488, MD Anderson Cancer Center, 1515 Holcombe Blvd, Houston, TX 77030; Michael T. Tetzlaff  mtetzlaff@mdanderson.org  Departments of Pathology and Translational and Molecular Pathology, Unit 85, MD Anderson Cancer Center, 1515 Holcombe Blvd, Houston, TX 77030

[#]These authors contributed equally to this work.

*These authors contributed equally to this work.

Color versions of one or more of the figures in the article can be found online at www.tandfonline.com/koni.

immune system against tumor cell antigens and have produced dramatic responses in cancers resistant to conventional systemic chemotherapies, including melanoma and Merkel cell carcinoma, both of which are aggressive cutaneous malignancies.^{15–17} Among the predictors of response to PD-1 inhibitors, PD-L1 expression by tumor cells and high levels of tumor-associated CD3-positive, CD8-positive (CD3+CD8+) T cells in pre-treatment or early on-treatment tumor biopsy samples correlate with clinical response to PD-1 or PD-L1 inhibitors.^{18–24}

Recent studies have associated the development of OASC with the integrity of the host immune system. Specifically, long-standing immunosuppression, including that related to solid organ transplant and HIV/AIDS, has been shown to be an important risk factor for the development of OASC.^{25–28} Therefore, given the paucity of effective therapeutic options for OASC beyond surgery together with the delicate anatomic location in the eye, the relationship between OASC and the immune system underscores an important unmet clinical need to determine if OASC might be amenable to immune checkpoint blockade. To this end, we sought to define the composition, density and spatial distribution of the tumor associated immune infiltrate in OASC and to ascertain whether OASC expresses PD-L1 to determine if the immune system might be reasonably leveraged to treat this aggressive ocular malignancy.

Results

Clinical features

Twenty-four primary OASCs from 24 patients, including 13 women and 11 men, were included in the final cohort. Patient characteristics and results of immunohistochemical staining are summarized in Table 1.

The median age at presentation was 69 years (range, 44–88 years). Sixteen specimens (67%) involved the upper eyelid, 7 (29%) involved the lower eyelid, 4 (17%) involved the conjunctiva, 4 (17%) involved the anterior orbit, and 2

(8%) involved the lacrimal gland/sac (6 specimens involved multiple anatomic locations). T category (AJCC 7th Edition; see methods) at presentation was T1 in 1 patient (4%), T2a in 2 patients (8%), T2b in 5 patients (21%), T3a in 8 patients (33%), T3b in 7 patients (29%), and not available in 1 patient (4%). Regional lymph node metastases were identified in 7 patients (29%), 3 of whom subsequently developed distant metastases in the liver (3 patients), lungs (2), and bones (1). The median follow-up time was 18 months (range, 2–87 months). At last follow-up, 20 patients were alive without evidence of disease, 1 patient had been lost to follow-up, and the 3 patients with distant metastases had died of their disease 19, 22, and 32 months after initial diagnosis.

Immunohistochemical stains of the immune infiltrate

PD-L1+ tumor cells were identified in 12 of the 24 specimens (50%). Overall, in our series of 24 primary OASCs, the density of the tumor-associated T-cell infiltrate was higher along the periphery of the tumor than in the center of the tumor for all of the markers assessed.

Relationship between the composition, density, and distribution of tumor-associated immune infiltrates and other clinical and pathologic variables

We found no association between sex, age, or tumor size and the density of immunohistochemical staining for CD3, CD8, PD-1, or FOXP3 in any position in the tumor. However, primary OASCs with T category of T3a or above in the AJCC staging system contained higher densities of CD3+, CD8+, and PD-1 + T cells at the tumor periphery than primary tumors with T category less than T3a (Table 2). Our findings were similar when considering the percentage of the immunohistochemically positive immune cells in a given area of tumor and tumor-associated stromal cells (considered as a binary variable – above or below the median for the population of tumors studied). Compared to primary OASCs with T category less than T3a, primary OASCs with T category of T3a or higher were more likely to have CD8 + T-cell density and PD-1 + T-cell density above the median at the tumor periphery, and a similar trend was observed for CD3 + T-cell density. Immune cell densities within the tumor center were not significantly associated with clinical (including T category) or pathologic variables, and the density of FOXP3+ immune cells and PD-L1 + tumor cells was not associated with T category.

When we considered metastatic disease progression, we did not observe any statistically significant differences in the density of the tumor associated immune infiltrates among primary OASCs that produced metastases compared to the primary OASCs that did not. (Table 2), suggestive that other features (molecular-genetic) drive disease progression in OASC.

Relationship between composition, density, and distribution of tumor-associated immune infiltrates and PD-L1 positivity

Given the previously described mechanism by which tumor-infiltrating T cells induce PD-L1 expression by tumor cells,²⁹

Table 1. Patient characteristics and immunohistochemical staining data for primary ocular adnexal sebaceous carcinomas^a.

Variable	N	Median	Min	Max
Age, years	24	69	44	88
Tumor size, mm	24	15	3	42
Time to lymph node metastases, months	7	9	0	21
Time to distant metastases, months	3	21	6	21
PD-L1-positive tumor cells, %	24	0.5	0.0	20.0
CD3 density				
At periphery	24	2258.38	149.03	4711.12
At center	17	230.30	11.98	2987.17
Total	24	1350.61	125.06	3358.39
CD8 density				
At periphery	24	932.90	27.95	2797.24
At center	17	59.90	9.32	1168.25
Total	24	572.20	27.95	2775.20
PD-1 density				
At periphery	24	400.08	19.92	2411.05
At center	17	59.79	5.32	510.90
Total	24	297.95	16.60	1277.31
FoxP3 density				
At periphery	23	308.87	13.31	1549.32
At center	17	51.87	0.00	1275.95
Total	23	200.52	19.31	1221.02

^a Values represent numbers of immunohistochemically positive cells per mm² unless otherwise specified.

Table 2. Association between immune parameters and AJCC (7th edition) T category at diagnosis or presence of metastases.

Immune parameter	N	Overall	≤T2b	≥T3a	P	No metastases	Metastases	P
Data analyzed as a continuous variable^a								
CD3 density								
At periphery	23	2182 (1442)	1076 (1050)	2773 (1282)	0.01	1826 (1411)	2997 (1241)	0.071
At center	16	456.0 (715.0)	261.2 (220.9)	544.5 (848.4)	0.692	275.7 (270.4)	756.4 (1108.6)	0.329
Total	23	1577 (1087)	956 (1059)	1908 (978)	0.061	1388 (1112)	2010 (963)	0.161
CD8 density								
At periphery	23	1162 (900)	566 (931)	1481 (726)	0.006	961 (900)	1623 (768)	0.071
At center	16	207.6 (337.5)	57.2 (38.0)	276.0 (392.2)	0.396	108.3 (174.6)	373.2 (484.0)	0.233
Total	23	873 (782)	531 (945)	1055 (641)	0.012	743 (760)	1170 (806)	0.142
PD-1 density								
At periphery	23	524.5 (531.5)	243.6 (222.3)	674.4 (591.6)	0.024	497.2 (575.1)	587.0 (450.0)	0.423
At center	16	123.0 (150.1)	59.3 (93.2)	151.9 (165.5)	0.282	103.7 (128.0)	155.1 (190.1)	0.515
Total	23	383.7 (325.1)	215.7 (227.1)	473.3 (340.0)	0.045	373.0 (351.0)	408.3 (280.2)	0.593
FOXP3 density								
At periphery	22	438.6 (460.3)	388.8 (528.4)	461.8 (443.1)	0.275	464.8 (504.5)	368.8 (343.7)	1
At center	16	161.3 (312.2)	114.7 (143.4)	182.5 (369.3)	0.777	99.1 (108.8)	265.0 (500.5)	0.914
Total	22	346.9 (387.8)	329.9 (464.7)	354.9 (364.4)	0.307	358.2 (391.4)	316.9 (413.0)	0.825
Data analyzed as a categorical variable^b								
PD-L1 status								
Negative	23				1.000			0.371
Positive		11 (47.8)	4 (50.0)	7 (46.7)		9 (56.2)	2 (28.6)	
		12 (52.2)	4 (50.0)	8 (53.3)		7 (43.8)	5 (71.4)	
CD3 status at periphery								
Above median	23	12 (52.2)	2 (25.0)	10 (66.7)	0.089	6 (37.5)	6 (85.7)	0.069
Below median		11 (47.8)	6 (75.0)	5 (33.3)		10 (62.5)	1 (14.3)	
CD3 status at center								
Above median	16	8 (50.0)	2 (40.0)	6 (54.5)	1.000	4 (40.0)	4 (66.7)	0.608
Below median		8 (50.0)	3 (60.0)	5 (45.5)		6 (60.0)	2 (33.3)	
CD3 status total								
Above median	23	12 (52.2)	2 (25.0)	10 (66.7)	0.089	7 (43.8)	5 (71.4)	0.371
Below median		11 (47.8)	6 (75.0)	5 (33.3)		9 (56.2)	2 (28.6)	
CD8 status at periphery								
Above median	23	12 (52.2)	1 (12.5)	11 (73.3)	0.009	6 (37.5)	6 (85.7)	0.069
Below median		11 (47.8)	7 (87.5)	4 (26.7)		10 (62.5)	1 (14.3)	
CD8 status at center								
Above median	16	8 (50.0)	2 (40.0)	6 (54.5)	1.000	4 (40.0)	4 (66.7)	0.608
Below median		8 (50.0)	3 (60.0)	5 (45.5)		6 (60.0)	2 (33.3)	
CD8 status total								
Above median	23	12 (52.2)	2 (25.0)	10 (66.7)	0.089	6 (37.5)	6 (85.7)	0.069
Below median		11 (47.8)	6 (75.0)	5 (33.3)		10 (62.5)	1 (14.3)	
PD-1 status at periphery								
Above median	23	12 (52.2)	1 (12.5)	11 (73.3)	0.009	7 (43.8)	5 (71.4)	0.371
Below median		11 (47.8)	7 (87.5)	4 (26.7)		9 (56.2)	2 (28.6)	
PD-1 status at center								
Above median	16	7 (43.8)	1 (20.0)	6 (54.5)	0.308	4 (40.0)	3 (50.0)	1.000
Below median		9 (56.2)	4 (80.0)	5 (45.5)		6 (60.0)	3 (50.0)	
PD-1 status total								
Above median	23	12 (52.2)	2 (25.0)	10 (66.7)	0.089	8 (50.0)	4 (57.1)	1.000
Below median		11 (47.8)	6 (75.0)	5 (33.3)		8 (50.0)	3 (42.9)	
FOXP3 status at periphery								
Above median	22	10 (45.5)	2 (28.6)	8 (53.3)	0.381	7 (43.8)	3 (50.0)	1.000
Below median		12 (54.5)	5 (71.4)	7 (46.7)		9 (56.2)	3 (50.0)	
FOXP3 status at center								
Above median	16	7 (43.8)	2 (40.0)	5 (45.5)	1.000	5 (50.0)	2 (33.3)	0.633
Below median		9 (56.2)	3 (60.0)	6 (54.5)		5 (50.0)	4 (66.7)	
FOXP3 status total								
Above median	22	10 (45.5)	2 (28.6)	8 (53.3)	0.381	8 (50.0)	2 (33.3)	0.646
Below median		12 (54.5)	5 (71.4)	7 (46.7)		8 (50.0)	4 (66.7)	

^aValues are mean (standard deviation) unless otherwise specified. *P* values are based on Wilcoxon rank-sum test for continuous variables.

^bValues are number (percentage) unless otherwise specified. *P* values are based on Fisher's exact test for categorical variables.

we examined whether PD-L1 expression by OASC tumor cells correlated with the density of the tumor-associated T-cell immune infiltrates and whether the spatial distribution of the tumor associated immune infiltrate also correlated with PD-L1 expression by tumor cells. When we examined this relationship, we observed that tumors expressing PD-L1 (staining of ≥1% of tumor cells) had significantly higher PD-1 + T-cell density along the tumor periphery compared to did tumors lacking PD-L1 expression (Table 3; Figure 2), and PD-1 expressing lymphocytes were enriched in geographic areas with higher tumor cell PD-L1 expression (Figure 2). No such association was observed between tumor

cell PD-L1 positivity and PD-1 + T-cell density in the tumor center, and no associations were observed between PD-L1 positivity in tumor cells and the density of tumor-associated CD3 + T cells, CD8 + T cells, or FOXP3 + T cells at the periphery or the center of the tumor).

Discussion

In the current study, we performed deep immune profiling and quantification of the tumor-associated immune infiltrate in a series of 24 primary OASCs. We demonstrated that a higher density of CD3+, CD8+, and PD-1 + T cells at the

Table 3. Association between immune parameters and tumor cell PD-L1 expression.

Immune parameter	N	Overall	Negative PD-L1 staining	Positive PD-L1 staining	P
Data analyzed as a continuous variable^a					
CD3 density					
At periphery	24	2106 (1460)	1686 (1592)	2526 (1239)	0.149
At center	17	429.9 (700.7)	283.2 (274.3)	560.2 (935.6)	0.923
Total	24	1519 (1101)	1217 (1113)	1820 (1047)	0.119
CD8 density					
At periphery	24	1119 (906)	976 (986)	1262 (836)	0.299
At center	17	196.0 (330.3)	123.2 (194.5)	260.6 (418.5)	0.773
Total	24	839.0 (782.3)	698.2 (712.5)	979.9 (853.5)	0.273
PD-1 density					
At periphery	24	505.2 (528.3)	280.0 (297.0)	730.5 (620.3)	0.021
At center	17	119.8 (145.9)	82.2 (131.0)	153.3 (157.8)	0.501
Total	24	370.4 (324.6)	246.6 (286.0)	494.3 (324.0)	0.038
FOXP3 density					
At periphery	23	439.5 (449.7)	378.1 (473.6)	506.4 (434.6)	0.356
At center	17	155.0 (303.4)	80.2 (115.8)	221.5 (402.3)	0.386
Total	23	343.0 (379.3)	244.9 (258.7)	450.0 (467.7)	0.268
Data analyzed as a categorical variable^b					
CD3 status at periphery					
Above median	24	12 (50.0)	4 (33.3)	8 (66.7)	0.220
Below median		12 (50.0)	8 (66.7)	4 (33.3)	
CD3 status at center					
Above median	17	8 (47.1)	3 (37.5)	5 (55.6)	0.637
Below median		9 (52.9)	5 (62.5)	4 (44.4)	
CD3 status total					
Above median	24	12 (50.0)	5 (41.7)	7 (58.3)	0.684
Below median		12 (50.0)	7 (58.3)	5 (41.7)	
CD8 status at periphery					
Above median	24	12 (50.0)	5 (41.7)	7 (58.3)	0.684
Below median		12 (50.0)	7 (58.3)	5 (41.7)	
CD8 status at center					
Above median	17	8 (47.1)	3 (37.5)	5 (55.6)	0.637
Below median		9 (52.9)	5 (62.5)	4 (44.4)	
CD8 status total					
Above median	24	12 (50.0)	5 (41.7)	7 (58.3)	0.684
Below median		12 (50.0)	7 (58.3)	5 (41.7)	
PD-1 status at periphery					
Above median	24	12 (50.0)	3 (25.0)	9 (75.0)	0.039
Below median		12 (50.0)	9 (75.0)	3 (25.0)	
PD-1 status at center					
Above median	17	8 (47.1)	2 (25.0)	6 (66.7)	0.153
Below median		9 (52.9)	6 (75.0)	3 (33.3)	
PD-1 status total					
Above median	24	12 (50.0)	4 (33.3)	8 (66.7)	0.220
Below median		12 (50.0)	8 (66.7)	4 (33.3)	
FOXP3 status at periphery					
Above median	23	11 (47.8)	6 (50.0)	5 (45.5)	1.000
Below median		12 (52.2)	6 (50.0)	6 (54.5)	
FOXP3 status at center					
Above median	17	8 (47.1)	3 (37.5)	5 (55.6)	0.637
Below median		9 (52.9)	5 (62.5)	4 (44.4)	
FOXP3 status total					
Above median	23	11 (47.8)	5 (41.7)	6 (54.5)	0.684
Below median		12 (52.2)	7 (58.3)	5 (45.5)	

^a Values are mean (standard deviation) unless otherwise specified. *P* values are based on Wilcoxon rank-sum test for continuous variables.

^b Values are number (percentage) unless otherwise specified. *P* values are based on Fisher's exact test for categorical variables.

tumor periphery was associated with higher AJCC T category. Further, we demonstrated that 50% of OASC specimens contained tumor cells expressing PD-L1, and these tumors were infiltrated by higher densities of PD-1 + T cells. Together, these observations suggest that the PD-1/PD-L1 axis is operational in a subset of primary OASCs, serving to inhibit the immune response and enable tumor progression, and further suggest that abrogation of the PD-1/PD-L1 axis through PD-1 blockade may be effective in the treatment of locally advanced or metastatic OASC.

The PD-1/PD-L1 axis has been studied extensively in recent years given the clinical application in treatment of metastatic cancer. PD-1 inhibitors have been approved by the US Food and Drug Administration for several historically treatment resistant solid tumors, including melanoma, renal

cell carcinoma, non-small cell lung carcinoma, head and neck squamous cell carcinoma, Merkel cell carcinoma, and Hodgkin lymphoma, and have produced impressive response rates.^{16,17,30–32} However, responses to PD-1 blockade remain challenging to predict, and only a few clinically available biomarkers predict response to these agents. Numerous reports have shown that PD-L1 expression by tumor cells in pretreatment biopsy specimens correlates with better responses to treatment with PD-1 inhibitors in melanoma and other cancers.^{29,33,34} Immunohistochemical assays for PD-L1 are thus used in clinical practice as predictors of response to anti-PD-1 therapy³¹ and, more important, to stratify melanoma patients for possible combination immune checkpoint blockade.³⁵ In addition, improved response to PD-1 blockade has been observed for tumors infiltrated by high

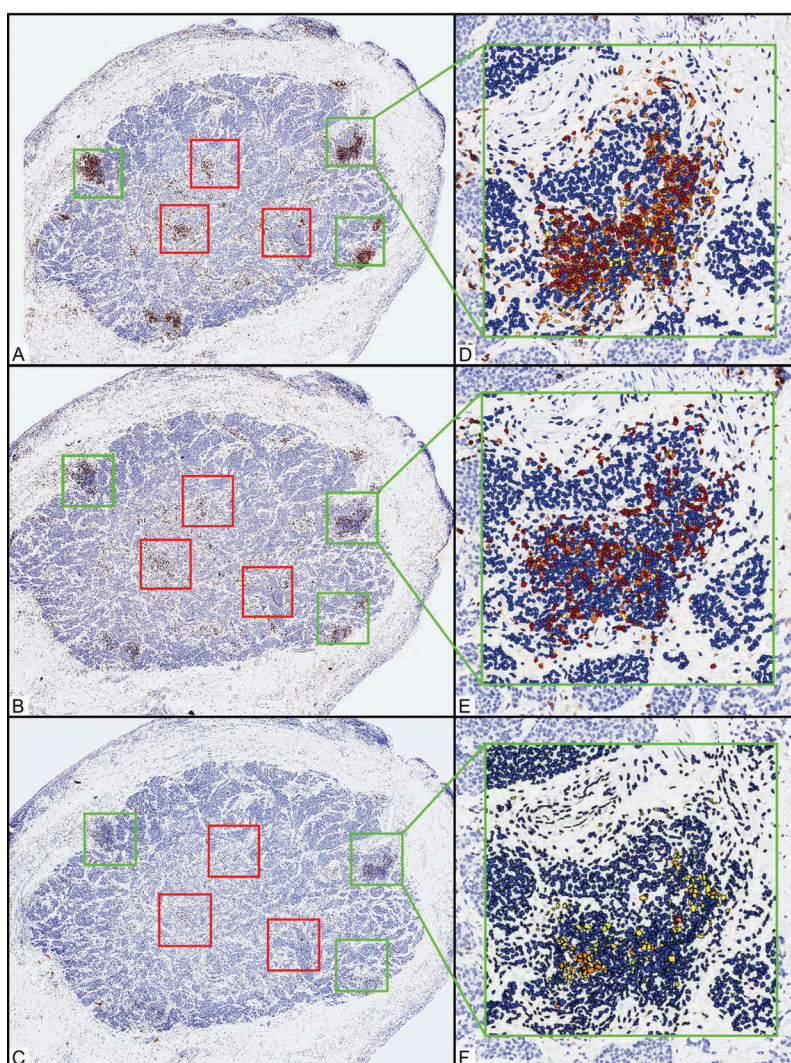


Figure 1. Representative example of quantification of the relative composition, density, and distribution of immune infiltrates in primary ocular adnexal sebaceous carcinoma. (A-C) Scanning magnification shows an ocular adnexal sebaceous carcinoma after immunohistochemical studies for CD3 (A, 40x), CD8 (B, 40x), and PD-1 (C, 40x). Green and red boxes delineate areas of the tumor in which the highest areas of immune cell density were assessed. Green boxes designate tumor periphery ($3 \times 0.25\text{-mm}^2$ boxes), and red boxes designate central areas ($3 \times 0.25\text{-mm}^2$ boxes). (D-F) Automated image analysis quantified the CD3-positive (CD3+) (D, 200x), CD8+ (E, 200x), and PD-1+ (F, 200x) cells. Immunohistochemically positive (IHC+) cells were quantified according to intensity (1+ yellow, 2+ orange, and 3+ brown), and cells with IHC-negative nuclei (including stromal and tumor cells) in a given area were counted and designated as a blue nucleus. IHC+ cells (including the sum of 1+, 2+, and 3+ cells) were tabulated and quantified as (1) number of IHC+ cells per 0.25 mm^2 or (2) percentage of the total nucleated cells in a given 0.25-mm^2 area.

levels of CD8 + T cells as measured in pretreatment and early-on-treatment biopsy specimens.^{23,36} Finally, high level of immune infiltration by CD3+ and CD8 + T cells is associated with improved survival of patients with colorectal and other cancer types (the basis for the “immunoscore”), showing a higher correlation with survival than the TNM stage in some studies.^{37,38}

PD-L1 has previously been shown to be expressed on melanoma cells and antigen-presenting cells at the tumor-stromal interface in a focal and geographically heterogeneous pattern.³⁹ We observed a similar pattern of geographically heterogeneous expression of PD-L1 in the tumor cells of our OASC specimens, with PD-L1 expression more common at the tumor-stromal interface than in the central region of the tumor. This observation is consistent with the previously described mechanism of PD-L1 induction by tumor-infiltrating T cells, in which engagement of PD-1 with PD-L1

mediates adaptive immune resistance in melanoma.^{31,40} In this context, T-cell activation occurs following exposure to tumor-specific antigens, and in response, activated T cells secrete IFN- γ and upregulate PD-1 expression. Both dendritic cells and tumor cells in the vicinity of these T cells then respond to IFN- γ by upregulating PD-L1 expression. The engagement of PD-1 with PD-L1 with results in suppression of T-cell activity. In our series of OASCs, the strong association between PD-L1+ tumor cells and PD-1 + T cells ($p = 0.021$) in the same geographically restricted regions that we analyzed (Figure 2) suggests T-cell-induced expression of PD-L1 on tumor cells.

The clinical relevance of our findings remains to be investigated in future studies using anti-PD-1 therapy in patients with locally advanced or metastatic sebaceous carcinoma. Taken together, our findings that (1) high levels of PD-1 + T cells correlated with PD-L1 expression in OASC

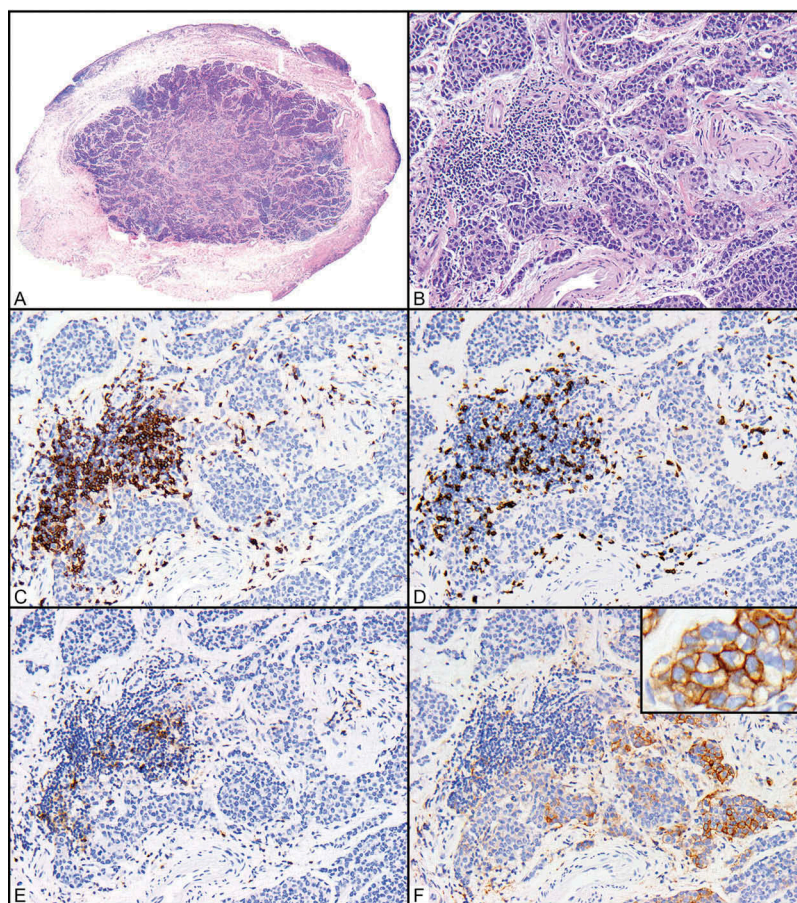


Figure 2. Relationships between CD3+, CD8+, and PD-1 + T cells and PD-L1-expressing tumor cells in a primary ocular adnexal sebaceous carcinoma. (A) Scanning magnification of an ocular adnexal sebaceous carcinoma (H&E, 40x). (B) Higher magnification shows infiltrating carcinoma in the same area where immunohistochemical positivity was quantified (H&E, 200x). (C-E) Antibodies for CD3 highlight a cluster of CD3-positive (CD3+) T cells associated with the tumor periphery (C, 200x), and a subset of these are CD8 + T cells (D, 200x) that also expressing PD-1 (E, 200x). (F) PD-L1+ tumor cells are seen in close proximity to these (F, 200x; inset 400x).

tumor cells and (2) high levels of CD3+, CD8+, and PD-1 + T cells at the tumor periphery (effectively a “suppressed T-cell phenotype” which would be permissive toward tumor progression) correlated with advanced AJCC T category, provide a compelling rationale for the application of PD-1 blockade in OASC. Further, it is envisioned that reversing this “suppressed T-cell phenotype” would likely unleash the endogenous immune response and might prove clinically beneficial to patients with OASC. We are aware of one anecdotal case report that is expected to be published soon (OPRS in press) of a patient with metastatic and locally advanced recurrent sebaceous carcinoma of the eyelid and orbit who responded to anti-PD1 therapy and based on findings in the current report plan to design a clinical trial to further investigate the efficacy of PD-1 inhibition for sebaceous carcinoma patients.

Whereas we found that more dense tumor-associated immune infiltrates correlated with higher T category in this study, most prior studies of other solid tumors have shown an inverse correlation between the density of the tumor-associated immune infiltrate and indices of patient outcome and survival, including stage.^{41,42} However, our findings may be analogous to similar observations in uveal melanoma, where tumors with monosomy for chromosome 3, which is associated with a higher risk for metastases, had a higher density

of tumor-associated lymphocytes than other subtypes.⁴³ Mechanisms proposed to explain this phenomenon include low density of tumor neoantigens, which contribute to the development of a T-cell response,⁴⁴ and an immune-privileged environment that suppresses the local immune response to the tumor.⁴⁵ In addition, the infiltrate we observed to correlate with advanced T category is a “suppressed T-cell infiltrate” consisting of CD3+ CD8+ PD-1 + T cells in geographic proximity to PD-L1 expression by both tumor cells and tumor-associated histiocytes. Thus, suppressed T-cell activity due to engagement between PD-1 and PD-L1 may additionally explain our observations. Another possible explanation is that smaller eyelid carcinomas do not have a high enough antigen load to instigate an immune-infiltrative response.

Treatment options for metastatic sebaceous carcinoma are currently limited and generally ineffective, underscoring the importance of identifying novel biomarkers or avenues for therapy. We previously reported whole-exome next-generation sequencing studies of cancer-associated genes in which we demonstrated that 45% of patients with OASC harbored somatically acquired mutations affecting potentially clinically actionable genes.⁴⁶ Specifically, we found frequent activation of the PI3K signaling pathway, implying the utility of PI3K

pathway inhibitors in the management of locally aggressive or metastatic OASC. Our finding in the current series of PD-1/PD-L1 expression in 50% of OASC tumor samples, the correlation of PD-1 expression by tumor-associated T cells with PD-L1 expression by tumor cells, and the higher densities of “suppressed” CD3+ CD8+ PD-1 + T-cell infiltrates in tumors with AJCC T category of T3a or greater together strongly suggest an additional potential role for immune checkpoint inhibitors for management of OASC, particularly locally advanced cases, in which tumor shrinkage due to neoadjuvant therapy might significantly reduce surgical morbidity. Future studies will assess possible clinical efficacy of this class of drugs for patients with OASC.

Materials and methods

The Institutional Review Board of The University of Texas MD Anderson Cancer Center approved this retrospective study. We searched the electronic medical records system of MD Anderson Cancer Center reviewed the pathology files to identify cases of primary OASC diagnosed and treated at our institution during 2007–2017. Of these cases, we included only cases of primary OASC for which pathological and clinical follow-up data and sufficient tissue for immunohistochemical studies were available.

The following clinical and pathologic variables were collected from patients’ medical records: age at presentation, sex, primary tumor site, tumor size, T category, and presence of regional or distant metastases. Staging criteria were applied at the time of this study according to the system for eyelid carcinoma in the seventh edition of the American Joint Commission on Cancer (AJCC) cancer staging manual.⁴⁷

Immunohistochemistry

Immunohistochemical studies were performed as previously described.³⁰ Briefly, a Leica Bond autostainer was used with the following antibodies and 3,3'-diaminobenzidine chromogen: CD3 (Dako A0452; 1:100), CD8 (Life Sciences Technologies MS457s; 1:25), FOXP3 (BioLegend 206D; 1:50), PD-1 (ABCAM ab137132; 1:250), and PD-L1 (Cell Signaling 13684S; 1:100).

Image analysis

Slides were scanned at 20x magnification on a digital slide scanner (Aperio AT Turbo; Leica Biosystems). Aperio ImageScope image analysis software (v12.3.2.8013) was used to quantify the number of positive cells within designated areas, as previously described.³⁰ Given the relatively small size of immune cells, a modified version of the Nuclear v9 algorithm was applied to determine immune marker positivity. Intensity thresholds were manually adjusted to remove background artifacts and to account for variable differences in cell size (especially for PD-L1).

Expression of CD3, CD8, PD-1, and FOXP3 was quantified in lymphocytes. For each marker, the tumor areas containing the highest densities of associated immunohistochemically positive cells were delineated with fixed squares, each with

an area of 0.25 mm² (0.5 x 0.5 mm). For each marker, up to 3 squares were drawn at the tumor periphery, defined as an approximately equal area of the leading edge of tumor cells and the adjacent stromal interface, and up to 3 squares were drawn in the tumor center, defined as central portions of the tumor separated from/not touching the tumor periphery) unassociated with peripheral aspects of the tumor. When the periphery or center of the tumor was too small to accommodate 3 × 0.25 mm² squares, then fewer 0.25-mm² squares, but as many as possible, were designated. For 7 cases in which the tumor surface area was insufficient for distinction of the periphery from the center, only the periphery was considered. In each square, the cells immunohistochemically positive for the marker of interest were digitally tabulated and summed, and the total number of positive cells was divided by the total area (in mm²) in which cells were counted (Figure 1). Immune cell densities were tabulated either as raw numbers (number of immunohistochemically positive cells/mm²) or as a percentage of the nucleated cells in the designated area.

Because PD-L1 expression on tumor cells is difficult to quantify using automated image analysis software owing to its membranous location and co-expression of PD-L1 on tumor-associated stromal cells, PD-L1+ tumor cells were counted manually, and results were reported as the percentage of PD-L1+ tumor cells.

Statistical analyses

We interrogated relationships between the composition, density, and distribution of the tumor-associated immune infiltrates and various clinical and pathologic variables. We also compared the composition, density, and distribution of the primary tumor-associated immune infiltrate between patients who developed metastatic OASC and those who did not. Categorical variables were summarized by frequencies and percentages, and continuous variables were summarized using means, standard deviations, medians, and ranges. Fisher’s exact test was used to assess associations between categorical variables, and Wilcoxon rank-sum test was used to assess the differences between groups. Pearson’s correlation coefficients were calculated to assess the associations between 2 continuous variables. Statistical analyses were performed using R version 3.3.1. All statistical tests used a significance level of 5%. No adjustments for multiple testing were made.

Acknowledgments

We thank Ms Stephanie Deming for help with medical editing. We thank Ms Kim Vu for her assistance with images and figures. MTT declares advisory board relationships with Novartis, Myriad Genetics and Seattle Genetics – all of which are unrelated to the current study.

Disclosure of Potential Conflicts of Interest

The authors declare no relevant conflicts of interest. MTT has unrelated advisory board relationships with Novartis, Myriad Genetics and Seattle Genetics.

ORCID

Oded Sagiv  <http://orcid.org/0000-0003-0563-278X>

Courtney W. Hudgens  <http://orcid.org/0000-0001-8312-7485>

References

- Mulay K, Aggarwal E, White VA. Periocular sebaceous gland carcinoma: A comprehensive review. *Saudi J Ophthalmol.* 2013;27:159–165. doi:10.1016/j.sjopt.2013.05.002.
- Pfeiffer ML, Savar A, Esmaeli B. Sentinel lymph node biopsy for eyelid and conjunctival tumors: what have we learned in the past decade? *Ophthal Plast Reconstr Surg.* 2013;29:57–62. doi:10.1097/IOP.0b013e31827472c5.
- Jakobiec FA, Mendoza PR. Eyelid sebaceous carcinoma: clinico-pathologic and multiparametric immunohistochemical analysis that includes adipophilin. *Am J Ophthalmol.* 2014;157:186–208. e2. doi:10.1016/j.ajo.2013.08.015.
- Shields JA, Saktanasate J, Lally SE, Carrasco JR, Shields CL. Sebaceous carcinoma of the ocular region: the 2014 professor winifred mao lecture. *Asia Pac J Ophthalmol (Philadelphia, Pa).* 2015;4:221–227. doi:10.1097/APO.0000000000000105.
- Nelson BR, Hamlet KR, Gillard M, Railan D, Johnson TM. Sebaceous carcinoma. *J Am Acad Dermatol.* 1995;33:1–15; quiz 6–8. doi:10.1016/0190-9622(95)90001-2.
- Eisen DB, Michael DJ. Sebaceous lesions and their associated syndromes: part I. *J Am Acad Dermatol.* 2009;61:549–60; quiz 61–2. doi:10.1016/j.jaad.2009.04.058.
- Dasgupta T, Wilson LD, Yu JB. A retrospective review of 1349 cases of sebaceous carcinoma. *Cancer.* 2009;115:158–165. doi:10.1002/cncr.23952.
- Shields JA, Demirci H, Marr BP, Eagle RC Jr., Shields CL. Sebaceous carcinoma of the eyelids: personal experience with 60 cases. *Ophthalmology.* 2004;111:2151–2157. doi:10.1016/j.ophtha.2004.07.031.
- Song A, Carter KD, Syed NA, Song J, Nerad JA. Sebaceous cell carcinoma of the ocular adnexa: clinical presentations, histopathology, and outcomes. *Ophthal Plast Reconstr Surg.* 2008;24:194–200. doi:10.1097/IOP.0b013e31816d925f.
- Rao NA, Hidayat AA, McLean IW, Zimmerman LE. Sebaceous carcinomas of the ocular adnexa: A clinicopathologic study of 104 cases, with five-year follow-up data. *Hum Pathol.* 1982;13:113–122. doi:10.1016/S0046-8177(82)80115-9.
- Chao AN, Shields CL, Krema H, Shields JA. Outcome of patients with periocular sebaceous gland carcinoma with and without conjunctival intraepithelial invasion. *Ophthalmology.* 2001;108:1877–1883. doi:10.1016/S0161-6420(01)00719-9.
- Esmaeli B, Nasser QJ, Cruz H, Fellman M, Warneke CL, Ivan D. American joint committee on cancer T category for eyelid sebaceous carcinoma correlates with nodal metastasis and survival. *Ophthalmology.* 2012;119:1078–1082. doi:10.1016/j.ophtha.2011.11.006.
- Butte MJ, Keir ME, Phamduy TB, Sharpe AH, Freeman GJ. Programmed death-1 ligand 1 interacts specifically with the B7-1 costimulatory molecule to inhibit T cell responses. *Immunity.* 2007;27:111–122. doi:10.1016/j.immuni.2007.05.016.
- Chen L. Co-inhibitory molecules of the B7-CD28 family in the control of T-cell immunity. *Nat Reviews Immunol.* 2004;4:336–347. doi:10.1038/nri1349.
- Schadendorf D, Hodi FS, Robert C, Weber JS, Margolin K, Hamid O, Patt D, Chen -T-T, Berman DM, Wolchok JD. Pooled analysis of long-term survival data from phase II and phase III trials of ipilimumab in unresectable or metastatic melanoma. *J Clin Oncol.* 2015;33:1889–1894. doi:10.1200/JCO.2014.56.2736.
- Hamid O, Robert C, Daud A, Hodi FS, Hwu W-J, Kefford R, Wolchok JD, Hersey P, Joseph RW, Weber JS, et al. Safety and tumor responses with lambrolizumab (anti-PD-1) in melanoma. *New England J Med.* 2013;369:134–144. doi:10.1056/NEJMoa1305133.
- Nghiem PT, Bhatia S, Lipson EJ, Kudchadkar RR, Miller NJ, Annamalai L, Berry S, Chartash EK, Daud A, Fling SP, et al. PD-1 blockade with pembrolizumab in advanced Merkel-cell carcinoma. *New England J Med.* 2016;374:2542–2552. doi:10.1056/NEJMoa1603702.
- Ma W, Gilligan BM, Yuan J, Li T. Current status and perspectives in translational biomarker research for PD-1/PD-L1 immune checkpoint blockade therapy. *J Hematol Oncol.* 2016;9:47. doi:10.1186/s13045-016-0277-y.
- Meng X, Huang Z, Teng F, Xing L, Yu J. Predictive biomarkers in PD-1/PD-L1 checkpoint blockade immunotherapy. *Cancer Treat Rev.* 2015;41:868–876. doi:10.1016/j.ctrv.2015.11.001.
- Paulson KG, Iyer JG, Simonson WT, Blom A, Thibodeau RM, Schmidt M, Pietromonaco S, Sokil M, Warton EM, Asgari MM, et al. CD8+ lymphocyte intratumoral infiltration as a stage-independent predictor of Merkel cell carcinoma survival: a population-based study. *Am J Clin Pathol.* 2014;142:452–458. doi:10.1309/AJCPKIDZM39CRPNC.
- Paulson KG, Iyer JG, Tegeder AR, Thibodeau R, Schelter J, Koba S, Schrama D, Simonson WT, Lemos BD, Byrd DR, et al. Transcriptome-wide studies of merkel cell carcinoma and validation of intratumoral CD8+ lymphocyte invasion as an independent predictor of survival. *J Clin Oncol.* 2011;29:1539–1546. doi:10.1200/JCO.2010.30.6308.
- Sihto H, Bohling T, Kavola H, Koljonen V, Salmi M, Jalkanen S, Joensuu H. Tumor infiltrating immune cells and outcome of Merkel cell carcinoma: a population-based study. *Clin Cancer Res.* 2012;18:2872–2881. doi:10.1158/1078-0432.CCR-11-3020.
- Tumeh PC, Harview CL, Yearley JH, Shintaku IP, Taylor EJ, Robert L, Chmielowski B, Spasic M, Henry G, Ciobanu V, et al. PD-1 blockade induces responses by inhibiting adaptive immune resistance. *Nature.* 2014;515:568–571. doi:10.1038/nature13954.
- Cottrell TR, Taube JM. PD-L1 and emerging biomarkers in immune checkpoint blockade therapy. *Cancer J (Sudbury, Mass).* 2018;24:41–46. doi:10.1097/PPO.0000000000000301.
- Lanoy E, Dores GM, Madeleine MM, Toro JR, Fraumeni JF Jr, Engels EA. Epidemiology of non-keratinocytic skin cancers among persons with acquired immunodeficiency syndrome in the US. *AIDS (London, England).* 2009;23:385. doi:10.1097/QAD.0b013e3283213046.
- Hoss E, Nelson SA, Sharma A. Sebaceous carcinoma in solid organ transplant recipients. *Int J Dermatol.* 2017;56:746–749. doi:10.1111/ijd.2017.56.issue-7.
- Zavos G, Karidis NP, Tsourouflis G, Bokus J, Diles K, Sotirchos G, Theodoropoulou E, Kostakis A. Nonmelanoma skin cancer after renal transplantation: a single-center experience in 1736 transplantations. *Int J Dermatol.* 2011;50:1496–1500. doi:10.1111/ijd.2011.50.issue-12.
- Imko-Walczuk B, Kryś A, Lizakowski S, Dębska-Ślizień A, Rutkowski B, Biernat W, Wojnarowska F. Sebaceous carcinoma in patients receiving long-term immunosuppressive treatment: case report and literature review. *Transplantation proceedings;* 2014; New York, NY: Elsevier Science, 2903–2907.
- Taube JM, Klein AP, Brahmer JR, Xu H, Pan X, Kim JH, Chen L, Pardoll DM, Topalian SL, Anders RA. Association of PD-1, PD-L1 ligands, and other features of the tumor immune microenvironment with response to anti-PD-1 therapy. *Clin Cancer Res.* 2014;20:5064–5074. doi:10.1158/1078-0432.CCR-13-3271.
- Feldmeyer L, Hudgens CW, Ray-Lyons G, Nagarajan P, Aung PP, Curry JL, Torres-Cabala CA, Mino B, Rodriguez-Canales J, Reuben A, et al. Density, distribution, and composition of immune infiltrates correlate with survival in merkel cell carcinoma. *Clin Cancer Res.* 2016;22:5553–5563. doi:10.1158/1078-0432.CCR-16-0392.
- Taube JM, Galon J, Sholl LM, Rodig SJ, Cottrell TR, Giraldo NA, Baras AS, Patel SS, Anders RA, Rimm DL, et al. Implications of the tumor immune microenvironment for staging and therapeutics. *Mod Pathol.* 2018;31:214–234. doi:10.1038/modpathol.2017.156.
- Kaufman HL, Russell J, Hamid O, Bhatia S, Terheyden P, D'Angelo SP, Shih KC, Lebbé C, Linette GP, Milella M, et al. Avelumab in patients with chemotherapy-refractory metastatic Merkel cell carcinoma: a multicentre, single-

- group, open-label, phase 2 trial. *Lancet Oncol.* 2016;17:1374–1385. doi:10.1016/S1470-2045(16)30364-3.
33. Weber JS, D'Angelo SP, Minor D, Hodi FS, Gutzmer R, Neyns B, Hoeller C, Khushalani NI, Miller WH, Lao CD, et al. Nivolumab versus chemotherapy in patients with advanced melanoma who progressed after anti-CTLA-4 treatment (CheckMate 037): a randomised, controlled, open-label, phase 3 trial. *Lancet Oncol.* 2015;16:375–384. doi:10.1016/S1470-2045(15)70076-8.
 34. Herbst RS, Soria J-C, Kowanetz M, Fine GD, Hamid O, Gordon MS, Sosman JA, McDermott DF, Powderly JD, Gettinger SN, et al. Predictive correlates of response to the anti-PD-L1 antibody MPDL3280A in cancer patients. *Nature.* 2014;515:563. doi:10.1038/nature14011.
 35. Larkin J, Chiarion-Sileni V, Gonzalez R, Grob JJ, Cowey CL, Lao CD, Schadendorf D, Dummer R, Smylie M, Rutkowski P, et al. Combined nivolumab and ipilimumab or monotherapy in untreated melanoma. *N Engl J Med.* 2015;373:23–34. doi:10.1056/NEJMoa1504030.
 36. Chen PL, Roh W, Reuben A, Cooper ZA, Spencer CN, Prieto PA, Miller JP, Bassett RL, Gopalakrishnan V, Wani K, et al. Analysis of immune signatures in longitudinal tumor samples yields insight into biomarkers of response and mechanisms of resistance to immune checkpoint blockade. *Cancer Discov.* 2016;6:827–837. doi:10.1158/2159-8290.CD-15-1545.
 37. Galon J, Costes A, Sanchez-Cabo F, Kirilovsky A, Mlecnik B, Lagorce-Pagès C, Tosolini M, Camus M, Berger A, Wind P, et al. Type, density, and location of immune cells within human colorectal tumors predict clinical outcome. *Science.* 2006;313:1960–1964. doi:10.1126/science.1129139.
 38. Galon J, Mlecnik B, Bindea G, Angell HK, Berger A, Lagorce C, Lugli A, Zlobec I, Hartmann A, Bifulco C, et al. Towards the introduction of the 'Immunoscore' in the classification of malignant tumours. *J Pathol.* 2014;232:199–209. doi:10.1002/path.4287.
 39. Sunshine JC, Nguyen PL, Kaunitz GJ, Cottrell TR, Berry S, Esandrio J, Xu H, Ogurtsova A, Bleich KB, Cornish TC, et al. PD-L1 expression in Melanoma: A quantitative immunohistochemical antibody comparison. *Clin Cancer Res.* 2017;23:4938–4944. doi:10.1158/1078-0432.CCR-16-1821.
 40. Taube JM, Anders RA, Young GD, Xu H, Sharma R, McMiller TL, Chen S, Klein AP, Pardoll DM, Topalian SL, et al. Colocalization of inflammatory response with B7-h1 expression in human melanocytic lesions supports an adaptive resistance mechanism of immune escape. *Sci Transl Med.* 2012;4:127ra37–ra37. doi:10.1126/scitranslmed.3003689.
 41. Mlecnik B, Tosolini M, Kirilovsky A, Berger A, Bindea G, Meatchi T, Bruneval P, Trajanoski Z, Fridman W-H, Pagès F, et al. Histopathologic-based prognostic factors of colorectal cancers are associated with the state of the local immune reaction. *J Clin Oncol.* 2011;29:610–618. doi:10.1200/JCO.2010.30.5425.
 42. Kirilovsky A, Marliot F, El Sissy C, Haicheur N, Galon J, Pages F. Rational bases for the use of the immunoscore in routine clinical settings as a prognostic and predictive biomarker in cancer patients. *Int Immunol.* 2016;28:373–382. doi:10.1093/intimm/dxw021.
 43. Bronkhorst IH, Vu TH, Jordanova ES, Luyten GP, Burg SH, Jager MJ. Different subsets of tumor-infiltrating lymphocytes correlate with macrophage influx and monosomy 3 in uveal melanoma. *Invest Ophthalmol Vis Sci.* 2012;53:5370–5378. doi:10.1167/iovs.11-9280.
 44. McGranahan N, Furness AJ, Rosenthal R, Ramskov S, Lyngaa R, Saini SK, Jamal-Hanjani M, Wilson GA, Birkbak NJ, Hiley CT, et al. Clonal neoantigens elicit T cell immunoreactivity and sensitivity to immune checkpoint blockade. *Science.* 2016;351:1463–1469. doi:10.1126/science.aaf1490.
 45. Niederkorn JY. Immune escape mechanisms of intraocular tumors. *Prog Retin Eye Res.* 2009;28:329–347. doi:10.1016/j.preteyeres.2009.06.002.
 46. Tetzlaff MT, Singh RR, Seviour EG, Curry JL, Hudgens CW, Bell D, Wimmer DA, Ning J, Czerniak BA, Zhang L, et al. Next-generation sequencing identifies high frequency of mutations in potentially clinically actionable genes in sebaceous carcinoma. *J Pathol.* 2016;240:84–95. doi:10.1002/path.4759.
 47. Edge S, Byrd D, Compton C, Fritz A, Greene F, Trotti A. *AJCC cancer staging handbook.* New York, NY: Springer; 2009.